LETTER

doi:10.1038/nature10352

# Recent decreases in fossil-fuel emissions of ethane and methane derived from firn air

Murat Aydin[1], Kristal R. Verhulst[1], Eric S. Saltzman[1], Mark O. Battle[2], Stephen A. Montzka[3], Donald R. Blake[1], Qi Tang[1] & Michael J. Prather[1]

**Methane and ethane are the most abundant hydrocarbons in the atmosphere and they affect both atmospheric chemistry and climate. Both gases are emitted from fossil fuels and biomass burning, whereas methane ($CH_4$) alone has large sources from wetlands, agriculture, landfills and waste water. Here we use measurements in firn (perennial snowpack) air from Greenland and Antarctica to reconstruct the atmospheric variability of ethane ($C_2H_6$) during the twentieth century. Ethane levels rose from early in the century until the 1980s, when the trend reversed, with a period of decline over the next 20 years. We find that this variability was primarily driven by changes in ethane emissions from fossil fuels; these emissions peaked in the 1960s and 1970s at 14–16 teragrams per year (1 Tg = $10^{12}$ g) and dropped to 8–10 Tg $yr^{-1}$ by the turn of the century. The reduction in fossil-fuel sources is probably related to changes in light hydrocarbon emissions associated with petroleum production and use. The ethane-based fossil-fuel emission history is strikingly different from bottom-up estimates of methane emissions from fossil-fuel use[1,2], and implies that the fossil-fuel source of methane started to decline in the 1980s and probably caused the late twentieth century slow-down in the growth rate of atmospheric methane[3,4].**

Ethane is an organic trace gas that is primarily emitted to the atmosphere during mining, processing, transport and consumption of fossil fuels, during use of biofuels, and during biomass burning[4–6]. It acts as a precursor of ozone and carbon monoxide in the troposphere. Ethane is oxidized rapidly by the hydroxyl radical ($OH^{\bullet}$) and has a seasonally varying lifetime (annual mean ~2 months). The short lifetime, coupled with a north–south asymmetry in its sources, leads to geographic and temporal variability in its atmospheric abundance[5,7]. Ethane abundance displays strong seasonal variability, with peak-to-peak amplitudes comparable to annual-mean levels. Annual-mean ethane levels are highest at high northern latitudes (HNL, that is, 30–90° N; 1.5 parts per billion) and lowest at high southern latitudes (HSL, that is, 30–90° S; 250 parts per trillion)[4].

We measured ethane in firn air collected at Summit (in Greenland), at the West Antarctic Ice Sheet – Divide, WAIS-D (in Antarctica), and at the South Pole. A synthesis inversion method was used to develop atmospheric histories of ethane for each site, using a one-dimensional firn air diffusion model (Fig. 1) (see Methods Summary). The mean temperatures and the ice accumulation rates are very similar at Summit (−31 °C, 20 cm $yr^{-1}$) and at WAIS-D (−31 °C, 22 cm $yr^{-1}$), resulting in similar gas age distributions in the firn and atmospheric histories constrained for the past 50–60 years (refs 8, 9). South Pole is considerably colder (−51 °C), with a lower ice accumulation rate (~8 cm $yr^{-1}$) and a deeper firn column. As a result, atmospheric histories based on South Pole firn air measurements are constrained for the past 80–90 years (ref. 10). The ethane atmospheric histories based on the WAIS-D and South Pole firn air measurements display the same trends for the period since 1950 (Fig. 1).

Mean annual ethane levels measured over Summit and South Pole are consistent with those at other high-latitude sites, indicating that the

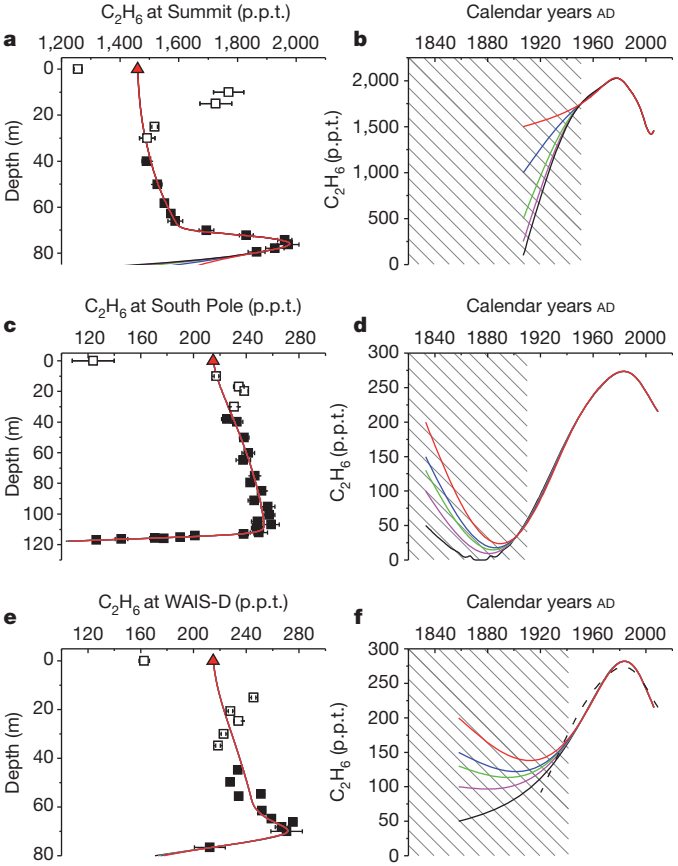


**Figure 1 | Ethane mixing ratios in firn air at three sites, and the atmospheric histories derived from these measurements.** **a**–**f**, Results for Summit (**a**, **b**), South Pole (**c**, **d**) and WAIS-D (**e**, **f**). Filled and open squares in **a**, **c** and **e** show measurements with estimated uncertainties (error bars, ±2 s.e.) (Supplementary Data). Solid lines in **a**, **c** and **e** show modelled firn profiles for the three respective sites, with the five different atmospheric histories (solid lines) shown in **b**, **d** and **f**. These five atmospheric histories were obtained by inverse modelling of the measurements with five different boundary conditions at $t_o$ that are identified by different colours, each representing a different pre-industrial mixing ratio for ethane. The data points in the top 35 m (Summit and South Pole) and 40 m (WAIS-D) of the firn are subject to the effects of seasonal variations in surface ethane levels (Supplementary Information) and are ignored during inverse modelling (open squares in **a**, **c** and **e**). The inversions were forced with contemporary annual-mean surface mixing ratios of 1,460 p.p.t. at Summit and 215 p.p.t. at South Pole and WAIS-D (red triangles in **a**, **c** and **e**) (Supplementary Information). The South Pole atmospheric history is overlaid on the independently derived WAIS-D atmospheric histories for comparison (dashed line in **f**). The inversions are sensitive to assumptions about the pre-industrial ethane levels before 1950, 1940 and 1910 at Summit, WAIS-D and South Pole, respectively (shaded areas), implying that only the inversion results for the later years are valid atmospheric histories.

[1]Department of Earth System Science, University of California, Irvine, California 92697, USA. [2]Department of Physics and Astronomy, Bowdoin College, Brunswick, Massachusetts 04011, USA. [3]Earth System Research Laboratories – Global Monitoring Division, National Oceanic and Atmospheric Administration, Boulder, Colorado 80305, USA.

measurements in polar firn air provide a reasonable sampling of the ethane mixing ratios in high latitudes (see Supplementary Information). Together, the three atmospheric histories show ethane levels peaking in the HNL and HSL atmospheres in the early 1980s, followed by a decline over the 20 years that followed. The South Pole site contains sufficiently old air to constrain the ramp-up period during the early to mid twentieth century (Fig. 1). On the basis of these atmospheric histories, HSL annual-mean ethane levels increased fivefold between 1910 and 1980 (from about 60 p.p.t. to 280 p.p.t.), and declined more than 10% (to less than 250 p.p.t.) by 2000. In the HNL, ethane increased from ~1.7 p.p.b. in 1950 to ~2.0 p.p.b. in 1980, and declined 25% to ~1.5 p.p.b. in 2000.

To infer the causes of the atmospheric ethane variations in terms of changes in large-scale sources, we must relate high-latitude ethane levels to hemispheric averages. We used the modern atmospheric ethane distribution[4,6] and sensitivity tests with the UCI Chemical Transport Model (UCI-CTM)[11,12] to derive ratios relating the response of the HNL and HSL to changes in hemispheric mean ethane levels (see Supplementary Information). Next, we used a simple two-box model (see Methods Summary) representing the troposphere in the Northern and Southern hemispheres to simulate variations in mean atmospheric ethane levels over the past century resulting from various scenarios for fossil-fuel, biomass-burning, and biofuel emissions. Fossil-fuel and biofuel emissions are concentrated in the northern mid-latitudes, and biomass burning in the tropics. As a result, these sources contribute to hemispheric ethane levels with different efficiencies (see Methods Summary and Supplementary Information).

The two-box model was used to infer the fossil-fuel ethane emission histories needed to achieve agreement with the firn-air-derived atmospheric ethane histories from Summit and South Pole, under various assumptions about biomass-burning emissions (Fig. 2, see Supplementary Information). The results show clearly that ethane variability over decadal timescales during the twentieth century was dominated by changes in the fossil-fuel ethane source. When biomass-burning and fossil-fuel ethane emissions are both allowed to vary after 1950, the model yields a biomass-burning source of less than 1 Tg yr$^{-1}$ in 1950, rising to ~3 Tg yr$^{-1}$ by 2000, followed by a drop to 2 Tg yr$^{-1}$. The model results show a large change in fossil-fuel ethane emissions in the first half of the twentieth century, peaking at 14–16 Tg yr$^{-1}$ in the late 1950s. Fossil-fuel emissions are then constant for about 20 years, followed by a 45% drop over the next 30 years. The model yields 8–10 Tg yr$^{-1}$ for fossil-fuel ethane emissions at the end of the twentieth century, consistent with the modern ethane budget inferred from atmospheric ethane levels[6,13].

Fossil-fuel emissions are also a significant source of methane into the atmosphere, and the observed decline in the growth rate of atmospheric methane[3,4] parallels the decline in atmospheric ethane levels during 1980–2000. This evidence suggests that the decline in methane growth rates was caused by a gradual reduction in fossil-fuel emissions, which was already underway when continuous direct atmospheric measurements of methane started in 1984 and 1985[3,4]. The stabilization of atmospheric ethane in recent years[4] (also see Supplementary Information) suggests that fossil-fuel emissions are now steady. Thus, the recent increases in atmospheric methane levels are probably not derived from increased fossil-fuel emissions and must be due to other sources, as previously suggested[14,15].

The ethane-based biomass-burning emission history agrees well with some independent estimates[6,16]. However, our fossil-fuel emissions history is quite different from bottom-up methane emission inventories[1,2] (Fig. 3). Most notably, the ethane-based fossil-fuel emissions display a steep ramp-up after 1920 and a sharp decline after 1980, whereas the bottom-up methane fossil-fuel emission inventories display a generally increasing trend through the entire twentieth century, with the sharpest increases occurring between 1950 and 1980. Hydrocarbons are emitted from a variety of fossil-fuel sources, each exhibiting a different range of methane/ethane emission ratio (MER). For example,

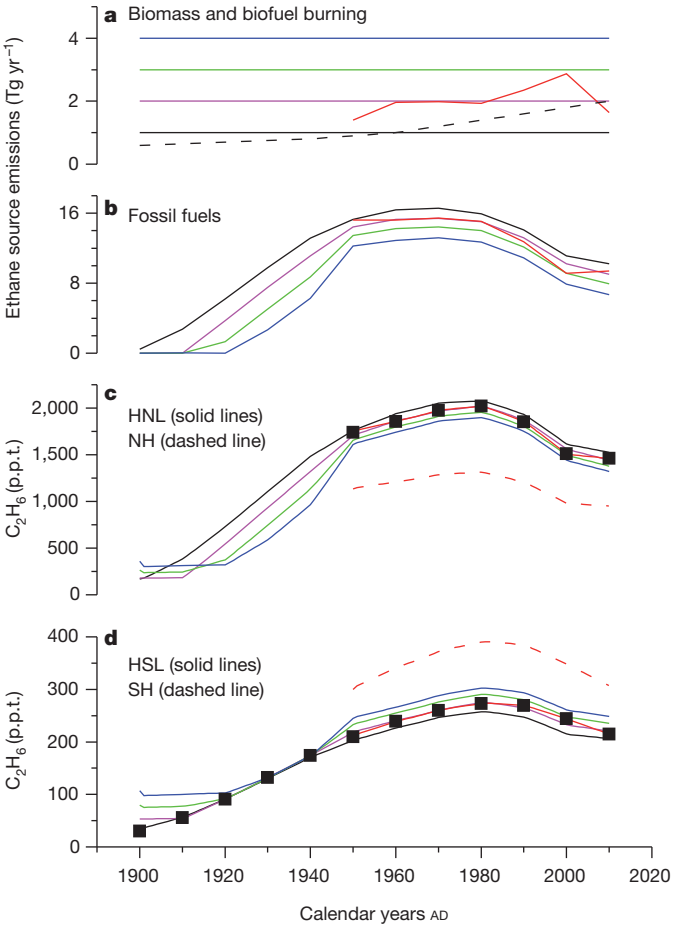


**Figure 2 | Ethane source emissions and the resulting atmospheric histories.** **a**–**d**, Historical global ethane emissions (**a**, **b**) and the resulting atmospheric histories (**c**, **d**) are derived with the two-box model to be consistent with the site-specific atmospheric histories based on firn-air results (Fig. 1). Fossil-fuel emission histories were developed by considering five different biomass-burning cases. In the first four cases, biomass-burning emissions are fixed at 1, 2, 3 and 4 Tg yr$^{-1}$ (black, purple, green and blue lines, respectively; **a**–**d**), and the fossil-fuel emissions are varied to minimize the $\chi^2$ value of the fit to the firn-air-based ethane atmospheric histories (black squares in **c** and **d**) from both the high northern latitudes and high southern latitudes (HNL and HSL) during 1950–2000, and from HSL only during 1900–1940. We included 2010 in the box model optimizations by assuming the atmospheric ethane levels remained constant at the mixing ratios used as surface tie-points used in firn inversions (Fig. 1). As a fifth case, the fit to the atmospheric histories is optimized by allowing both the fossil-fuel and the biomass-burning emissions to vary (thick red lines). Variable biomass burning is considered only for the period since 1950, because atmospheric histories from both hemispheres are needed to constrain the partitioning between fossil-fuel and biomass-burning emissions. Emissions from biofuel burning are fixed at the historical estimates (dashed black line; **a**) in all five cases[2]. The atmospheric lifetime of ethane (Methods Summary) is also the same in all five cases. The hemispheric-average atmospheric histories are also shown for the fifth case (dashed red lines; **c** and **d**), in which fossil-fuel and biomass-burning emissions are both varied. Ethane levels in HNL and HSL are obtained from Northern and Southern hemispheric (NH and SH) levels using the following ratios for fossil-fuel, biofuels and biomass-burning emissions: HNL/NH: 1.6, 1.4, 1.0; HSL/SH: 0.7, 0.7, 0.7. Values differ from 1.0 owing to the latitudinal distribution of each type of emission (Supplementary Information).

coal and natural gas emissions are methane-rich (MER = 5–100) with respect to emission ratios measured near oil-storage and oil-processing facilities (MER = 3–5)[6]. It is possible that the global-average MER (the ratio of total methane to total ethane emissions from all fossil-fuel sources combined) changed over time as the relative emission strengths of the different fossil-fuel sources varied during the twentieth century,

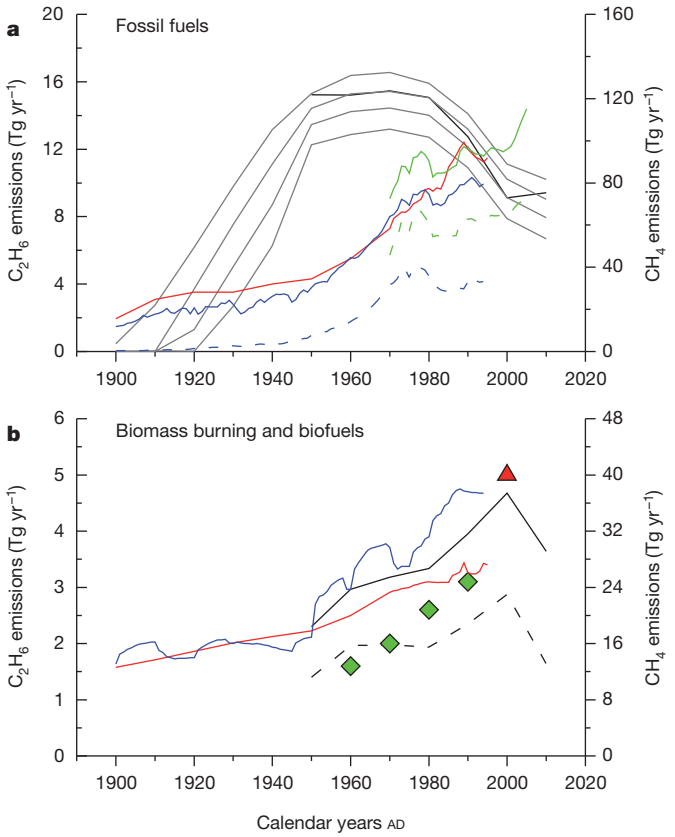


**Figure 3 | Ethane and methane emissions from fossil fuels, biofuels and biomass burning. a**, Ethane-based fossil-fuel emission histories (left *y*-axis) for fixed biomass burning (solid grey lines) and variable biomass burning (solid black line) cases, compared with bottom-up methane emission estimates from fossil fuels (coloured lines, right *y*-axis) based on the following sums of emissions: blue, gas flaring, gas supply and coal mining[1]; red, fossil-fuel consumption, fossil-fuel production and industrial[2]; green, oil, gas and solid fuels (data from http://edgar.jrc.ec.europa.eu/). The oil and gas only methane emissions from EDGAR4.1 (see URL in previous sentence; green dashed line) and gas flaring and gas supply methane emissions from ref. 1 (blue dashed line) are also shown. The trends in the ethane-based histories are relatively insensitive to assumptions about biomass burning. None of the bottom-up methane fossil-fuel emission inventories display a persistent decline during 1980–2000 that would be consistent with the ethane-based emission histories. The scales of the left and right *y*-axes are set at a ratio of 8 because it suits the presentation well and is consistent with **b**. **b**, Ethane emissions (left *y*-axis) from biomass burning (dashed black line) and biomass-burning+biofuels (solid black line) for the variable biomass-burning case in the two-box model compared with methane emissions (right *y*-axis) attributed to the total burning product from ref. 1 (blue line)[1] and with EDGAR-HYDE 1.4 (red line)[2]. The scales of the left and right *y*-axes are set at a ratio of 8, which is a measurement-based estimate of methane/ethane emission ratio (MER) from biomass burning[30]. Our results and the bottom-up methane inventories are consistent in how hydrocarbon emissions from biomass burning changed over time and suggest an MER of 8 on a Tg per Tg basis, in agreement with the earlier estimates[30]. Our estimate of ethane biomass-burning emissions from the variable biomass-burning case is also in good agreement with some independent estimates of historical ethane emissions from biomass burning[16] (green diamonds, left *y*-axis) and a total burning emissions estimate (biomass burning+biofuels) for present day[6] (red triangle, left *y*-axis).

but the apparent differences between the ethane-based fossil-fuel emission histories and inventory-based methane emissions (Fig. 3) cannot be reconciled with such considerations. Inconsistencies are already apparent in mid-century, when the ratio of bottom-up methane emissions to ethane-based fossil-fuel emissions imply an MER of 2–3 (Fig. 3). It is highly unlikely that the global-average MER during the 1950s could be lower than point sources with the lowest MERs, especially considering that both coal and natural gas were sources of significant hydrocarbon emissions during that period. This suggests the bottom-up methane inventories underestimate fossil-fuel emissions at mid-century.

The ethane-based estimates of fossil-fuel emissions show a decline during the 1980s, while the methane-inventory-based estimates of fossil-fuel emissions show an increase (Fig. 3). Opposing trends in the fossil-fuel emissions of ethane and methane are highly unlikely, because this requires ethane to be selectively removed from both newly introduced and existing hydrocarbon sources while the residual methane is released to the atmosphere. Natural gas is used in the production of feedstock ethane in plastics manufacturing. However, it seems implausible that methane, which is economically the most valuable component of natural gas, would simply be vented back into the atmosphere after ethane had been removed from natural gas. In fact, the amount of feedstock ethane produced from natural gas is inversely related to the price of natural gas[17], and probably declined as natural gas became progressively more valuable during the second half of the twentieth century. We conclude that the discrepancy between the ethane-based fossil-fuel emission histories and the fossil-fuel emission histories from the bottom-up methane inventories cannot be explained by realistic changes in global-average MER during the twentieth century.

The decline in fossil-fuel emissions, as calculated from our firn-air ethane records, coincides with a period of rapid expansion in natural gas production during the second half of the twentieth century[18,19]. We speculate that the rising economic value of natural gas during the late twentieth century[19] and the development of cleaner technologies led to sharp reductions in the release of light hydrocarbons into the atmosphere. Emissions linked specifically to the growing natural gas industry must have been more than offset by large reductions in the venting of light hydrocarbons, including methane and ethane, associated with production and processing of petroleum. These changes appear to be underestimated in the bottom-up methane inventories. We estimate that the total decline in fossil-fuel emissions of ethane was 5–6 Tg yr$^{-1}$ during 1980–2000. Attributing this decline entirely to decreases in fossil-fuel emission sources with the lowest MER (3–5) implies a 15–30 Tg yr$^{-1}$ drop in fossil-fuel emissions of methane. Distributing the decline among different fossil-fuel sources would yield a larger change in methane emissions from fossil fuels. An independent inversion analysis of methane observations suggests that a 20 Tg yr$^{-1}$ drop in fossil-fuel methane emissions during the 1990s contributed to the decline in methane growth rates[20]. Our results are consistent with such a decline, but provide additional evidence that the drop in fossil-fuel emissions started sooner, by about a decade. The decline in fossil-fuel emissions during the 1990s accounts for less than 60% of the total reduction during 1980–2000 in the two-box model results for ethane, suggesting that the reduction in fossil-fuel methane emissions could be ~40% larger than the previous estimate[20] of 20 Tg yr$^{-1}$.

Given that we do not have comparable observations from lower latitudes, it is possible that a shift in the location of fossil-fuel emissions towards lower latitudes within the Northern Hemisphere contributed to the observed ethane decline during 1980–2000. However, we estimate this effect to be relatively small on the basis of sensitivity tests with the UCI-CTM, which show that possible changes in the location of the emission reductions for ethane could add about 20% to the magnitude of emission reductions calculated above (see Supplementary Information).

It is also possible that the late twentieth century decline in ethane could have been caused by a decrease in the atmospheric lifetime of ethane, but we estimate the likelihood for such changes to be low. Assuming fixed emissions, a 5–6 Tg yr$^{-1}$ increase in ethane loss (roughly one-third of the peak budget) would be required to account for the observed ethane decline. A change of this magnitude due to increases in OH$^{\bullet}$ concentrations during the late twentieth century is unlikely[21,22]; however, atmospheric levels of chlorine atoms (Cl$^{\bullet}$) might have increased, because of increasing tropospheric $NO_x$, increasing tropospheric ozone and increasing acidity of aerosols[23,24]. A Cl$^{\bullet}$ sink

of the magnitude required to explain the ethane decline would have a minor effect on the methane budget (~3%), because the relative reactivity of $Cl^{\bullet}$ versus $OH^{\bullet}$ ($k_{Cl}/k_{OH}$) is considerably smaller for methane than it is for ethane. Accounting for the ethane decline would require an increase of roughly $1.1 \times 10^4$ $Cl^{\bullet}$ $cm^{-3}$ over the entire marine boundary layer, or a much larger increase if just the polluted boundary layer is considered. Estimates for the clean marine boundary layer are in the range $10^3$–$10^4$ $Cl^{\bullet}$ $cm^{-3}$. It is not possible to assess whether a change of the required magnitude is viable with the limited observational data available at present[23,25].

## METHODS SUMMARY

**Firn-air measurements, modelling and inversion.** At all three sites, multiple flasks (see Supplementary Information) from the same depth were filled sequentially, using established methods[10]. All flasks were analysed at the University of California, Irvine, using ~100 $cm^3$ STP samples on a gas chromatography-mass spectrometry (GC-MS) system designed for trace gas analysis on small air samples[26]. Summit and South Pole flasks were analysed at least twice. We used a one-dimensional firn-air model and a synthesis inversion method to derive atmospheric histories of the annual-mean, high-latitude, tropospheric abundances of ethane from the firn-air measurements (see Supplementary Information).

**Two-box model.** The Northern and Southern hemispheres are represented as equal mass boxes of $2.2 \times 10^9$ Tg (exchange time 1 year). Ethane is lost through $OH^{\bullet}$ oxidation ($^1/_{2.6}$ $months^{-1}$) and transport into the stratosphere ($^1/_{35}$ $yr^{-1}$), yielding a present day lifetime of 2.3 months. The annual-mean $OH^{\bullet}$ loss frequency varies over the past 100 years based on the methane feedback on tropospheric $OH^{\bullet}$: −0.32% in $OH^{\bullet}$ for every +1% in methane[27]. The $OH^{\bullet}$ changes differently in Northern and Southern hemispheres: −0.305% and −0.335%, respectively, based on simulations with the UCI-CTM[11,12]. We adopt a methane increase of 900 p.p.b. to 1,790 p.p.b. since 1900[28]. Fossil-fuel, biofuel and biomass-burning sources in the model Northern Hemisphere are adopted from previous work[6] and represent 93%, 81% and 58%, respectively, of the total emissions. The fossil-fuel emission histories for various biomass-burning scenarios are developed by an inverse optimization algorithm (see Supplementary Information).

**Three-dimensional model.** The UCI-CTM's simulation of ethane with realistic distribution of sources[29] is used to relate the northern and southern tropospheric mean abundances to the annual-mean abundance over the ice sheets, and thus provide a correction to the two-box model histories for the firn-air modelling.

**Received 15 September 2010; accepted 6 July 2011.**


1. Stern, D. I. & Kaufmann, R. K. Estimates of global anthropogenic methane emissions 1860–1993. *Chemosphere* **33,** 159–176 (1996).
2. van Aardenne, J. A., Dentener, F. J., Olivier, J. G. J., Klein Goldewijk, C. G. M. & Lelieveld, J. A. 1°x1° resolution data set of historical anthropogenic trace gas emissions for the period 1890–1990. *Glob. Biogeochem. Cycles* **15,** 909–928 (2001).
3. Dlugokencky, E. J. *et al.* Atmospheric methane levels off: temporary pause or a new steady-state? *Geophys. Res. Lett.* **30,** 1992, doi:10.1029/2003GL018126 (2003).
4. Simpson, I. J., Rowland, F. S., Meinardi, S. & Blake, D. R. Influence of biomass burning during recent fluctuations in the slow growth of global tropospheric methane. *Geophys. Res. Lett.* **33,** L22808, doi:10.1029/2006GL027330 (2006).
5. Rudolph, J. The tropospheric distribution and budget of ethane. *J. Geophys. Res.* **100,** 11369–11381 (1995).
6. Xiao, Y. *et al.* Global budget of ethane and regional constraints on U.S. sources. *J. Geophys. Res.* **113,** D21306, doi:10.1029/2007JD009415 (2008).
7. Boissard, C., Bonsang, B., Kanakidou, M. & Lambert, G. TROPOZ II: global distributions and budgets of methane and light hydrocarbons. *J. Atmos. Chem.* **25,** 115–148 (1996).
8. Aydin, M. *et al.* Post-coring entrapment of modern air in some shallow ice cores collected near the firn-ice transition: evidence from CFC-12 measurements in Antarctic firn air and ice cores. *Atmos. Chem. Phys.* **10,** 5135–5144 (2010).
9. Faïn, X. *et al.* Mercury in the snow and firn at Summit Station, Central Greenland, and implications for the study of past atmospheric mercury levels. *Atmos. Chem. Phys.* **8,** 3441–3457 (2008).
10. Battle, M. *et al.* Atmospheric gas concentrations over the past century measured in air from firn at the South Pole. *Nature* **383,** 231–235 (1996).
11. Hsu, J., Prather, M. J. & Wild, O. Diagnosing the stratosphere-to-troposphere flux of ozone in a chemistry transport model. *J. Geophys. Res.* **110,** D19305, doi:10.1029/2005JD006045 (2005).
12. Prather, M. J., Zhu, X., Strahan, S. E., Steenrod, S. D. & Rodriguez, J. M. Quantifying errors in trace gas species transport modeling. *Proc. Natl Acad. Sci. USA* **105,** 19617–19621 (2008).
13. Pozzer, A. *et al.* Observed and simulated global distribution and budget of atmospheric $C_2$-$C_5$ alkanes. *Atmos. Chem. Phys.* **10,** 4403–4422 (2010).
14. Dlugokencky, E. J. *et al.* Observational constraints on recent increases in the atmospheric $CH_4$ burden. *Geophys. Res. Lett.* **36,** L18803, doi:10.1029/2009GL039780 (2009).
15. Rigby, M. *et al.* Renewed growth of atmospheric methane. *Geophys. Res. Lett.* **35,** L22805, doi:10.1029/2008GL036037 (2008).
16. Schultz, M. G. *et al.* Global wildland fire emissions from 1960 to 2000. *Glob. Biogeochem. Cycles* **22,** GB2002, doi:10.1029/2007GB003031 (2008).
17. Remer, D. S. & Jorgens, C. Ethylene economics and production forecasting in a changing environment. *Eng. Process Econ.* **3,** 267–278 (1978).
18. Barns, D. W. & Edmonds, J. A. *An Evaluation of the Relationship Between the Production and Use of Energy and Atmospheric Methane Emissions* (TR047, DOE/NBB-0088P, National Technical Information Service, US Dept of Commerce, Springfield, 1990).
19. Gilardoni, A. *The World Market for Natural Gas; Implications for Europe* (Springer, 2008).
20. Bousquet, P. *et al.* Contribution of anthropogenic and natural sources to atmospheric methane variability. *Nature* **443,** 439–443 (2006).
21. Prinn, R. G. *et al.* Evidence for variability of atmospheric hydroxyl radicals over the past quarter century. *Geophys. Res. Lett.* **32,** L07809, doi:10.1029/2004GL022228 (2005).
22. Montzka, S. A. *et al.* Small interannual variability of global atmospheric hydroxyl. *Science* **331,** 67–69 (2011).
23. Lawler, M. J. *et al.* Pollution-enhanced reactive chlorine chemistry in the eastern tropical Atlantic boundary layer. *Geophys. Res. Lett.* **36,** L08810, doi:10.1029/2008GL036666 (2009).
24. Thornton, J. A. *et al.* A large atomic chlorine source inferred from mid-continental reactive nitrogen chemistry. *Nature* **464,** 271–274 (2010).
25. Allan, W., Struthers, H. & Lowe, D. C. Methane carbon isotope effects caused by atomic chlorine in the marine boundary layer: global model results compared with southern hemisphere measurements. *J. Geophys. Res.* **112,** D04306, doi:10.1029/2006JD007369 (2007).
26. Aydin, M., Williams, M. B. & Saltzman, E. S. Feasibility of reconstructing paleoatmopsheric records of selected alkanes, methyl halides, and sulfur gases from Greenland ice cores. *J. Geophys. Res.* **112,** D07312, doi:10.1029/2006JD008027 (2007).
27. Prather, M. *et al.* in *Climate Change 2001: The Scientific Basis* (eds Hougton, J. T. *et al.*) (Cambridge Univ. Press, 2001).
28. MacFarling Meure, C. *et al.* Law Dome $CO_2$, $CH_4$, and $N_2O$ ice core records extended to 2000 years BP. *Geophys. Res. Lett.* **33,** L14810, doi:10.1029/2006GL026152 (2006).
29. Tang, Q. & Prather, M. J. Correlating tropospheric column ozone with tropopause folds: the Aura-OMI satellite data. *Atmos. Chem. Phys.* **10,** 9681–9688 (2010).
30. Andreae, M. O. & Merlet, P. Emission of trace gases and aerosols from biomass burning. *Glob. Biogeochem. Cycles* **15,** 955–966 (2001).


**Supplementary Information** is linked to the online version of the paper at www.nature.com/nature.

**Acknowledgements** We thank T. Sowers, M. Drier and ICDS drillers for support during firn-air sampling and drilling in the field, and T. Sowers for discussions during preparation of the manuscript. We thank M. Bender and J. Severinghaus for $^{15}N$ measurements in firn air, S. Meinardi for ethane measurements in surface flasks, and P. Tans and P. Lang for firn-air $CO_2$ data. This work was supported by the National Science Foundation (grants ANT-0739598, ANT-0440602, ANT-0440509, ARC-0520460) and NASA (grant NAG58935).

**Author Contributions** M.A.: firn-air sampling, ethane analysis in firn air and surface-air flasks, firn-air modelling, two-box modelling, box-model inversions, manuscript preparation. K.R.V.: ethane analysis in firn air and surface-air flasks, firn-air modelling, two-box modelling, firn-air and two-box model inversions, manuscript improvements. E.S.S.: firn-air modelling, two-box modelling, firn-air and two-box model inversions, manuscript improvements. M.O.B.: firn-air sampling, firn-air modelling, manuscript improvements. S.A.M.: halocarbon measurements in firn air to constrain firn processes, NOAA surface air samples, manuscript improvements. D.R.B.: ethane measurements in surface air, manuscript improvements. Q.T.: CTM modelling, manuscript improvements. M.J.P.: CTM modelling, manuscript improvements.

**Author Information** Reprints and permissions information is available at www.nature.com/reprints. The authors declare no competing financial interests. Readers are welcome to comment on the online version of this article at www.nature.com/nature. Correspondence and requests for materials should be addressed to M.A. (maydin@uci.edu).